# Carbon Dioxide Storage in Stable Carbonate Minerals

Basalt Laboratory Studies of Interest to Carbon Capture and Storage April 29

2011

Adam Farrell; Advisor MN Evans University of Maryland Geology 394

#### **Abstract**

Among the various CCS technologies, storing  $CO_2$  as mineral carbonates in mafic rocks is being examined as a means to sequester  $CO_2$  over geologically significant time scales. In this study, powdered basalt from the Boring Lava Field of Washington State was reacted with  $CO_2$  in aqueous solution at conditions of 150 bar and  $150^{\circ}$  C. Three grain sizes were tested: 425-250um, 250-180um, and <180um. Each reaction took place over two weeks. Dissolution of calcium oxide, precipitation of calcite, and a net consumption of  $CO_2$  were observed and analyzed using two methods: calculated mass difference and chemical analysis in an Elemental Analyzer. Mass difference calculations revealed  $CO_2$  capture on the order of 3-8%, which is consistent with the reactions of Garcia et al. (2010) and other studies. Elemental analysis reflects these conclusions and offers other insights into grain size and capture yield. Both methods of analysis reveal significant, reproducible carbonate yields and an expected inverse relationship between carbonate yield and grain size. Although this and other CCS Strategies are geologically feasible, the financial considerations make this technology unlikely for significant utility scale development until capture technologies improve and carbon emissions are regulated.

#### **Abbreviations:**

Gt – Gigaton, 10<sup>9</sup> tons

 $Mt - Megaton, 10^6 tons$ 

CCS – Carbon Capture and Storage (or sequestration)

CO<sub>2</sub> – Carbon dioxide

GHG – Greenhouse gas

XRF – X-ray fluorescence spectroscopy

bar – Unit of pressure equal to 100 kilopascals

Mw – Megawatt, 10<sup>6</sup> watts

pCO<sub>2</sub> – Partial pressure due to CO<sub>2</sub>

pH<sub>2</sub>0 – Partial pressure due to H<sub>2</sub>0

SA – Surface area

# **Table of Contents**

TITLE PAGE	1
ABSTRACT AND ABBREVIATIONS	2
TABLE OF CONTENTS	3
LIST OF FIGURES	4
INTRODUCTION	5
METHOD OF ANALYSIS AND HYPOTHESES	7
EXPERIMENTAL DESIGN	9
PRESENTATION OF DATA	11
DISCUSSION OF RESULTS	15
ANALYSIS OF UNCERTAINTY	16
SUGGESTIONS FOR FUTURE WORK	17
CONCLUSIONS	17
DISCUSSION	18
AKNOWLEDGEMENTS	19
BIBLIOGRAPHY	20
APPENDICES	22

# **List of Figures**

Figure 1 US CO2 Emissions by Source	2
Figure 2 CO2 Trapping Mechanism Stability	5
Table 1 CO2 Programs capturing > 1Mt CO <sub>2</sub> annually	6
Figure 3 Sample of vesicular basalt	7
Table 2 Table showing relationships between surface area and grain size	7
Table 3 XRF sample data	8
Figure 4 Percentage of CO <sub>2</sub> trapped as carbonate. From Garcia et al., 2010	9
Table 4 Masses of reactants and products, and mass difference analysis	11
Table 5 Calculations and analyses of mass data	11
Figure 5 Sample mass increase vs. average grain size	12
Figure 6 Average mass increase vs. relative surface areas	12
Table 6 Elemental Analyzer Results.	13
Figure 7 Average grain size vs. % carbon.	14
Figure 8 Relative Surface Area vs. Average % Carbon by Mass	14
Table 7 Uncertainty values for instruments used during trials.	16
Table 8 Locations of future CO <sub>2</sub> injection sites.	17
Figure 9 Results of reactive-transport calculations.	19

#### Introduction

Cheap and abundant fossil fuels will remain a significant power generation source for dozens of years both domestically and abroad. Climate change models and reports show significant temperature increases within the next 100 years at current and increasing rates of emission of greenhouse gases (GHG). Carbon Capture and Storage (CCS) technologies present one method of maintaining or increasing United States electric power generation while minimizing CO<sub>2</sub> emissions from this sector (Meehl et al, 2007). Global energy consumption relies heavily on fossil fuels for both the power generation and transportation industries. The

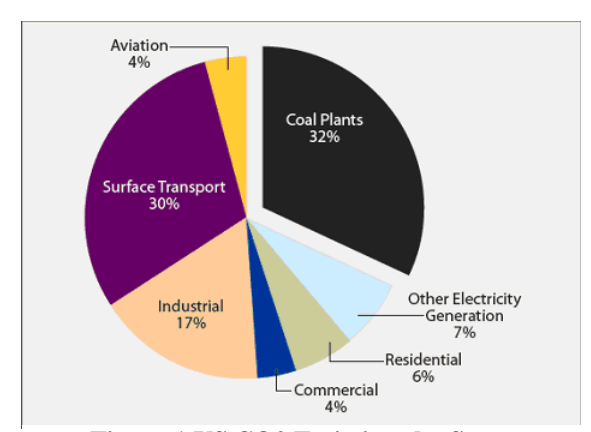


Figure 1 US CO2 Emissions by Source.

combustion of these fuels releases carbon dioxide into the atmosphere, with annual amounts totaling over 25Gt worldwide (Friedmann, 2007). As evidenced by Figure 1, fossil fuel power generation is responsible for nearly 40% of current  $CO_2$  emissions. With growing population and industrialization, the amount of  $CO_2$  produced is projected to grow steadily to over 95 Gt  $CO_2$  released annually by 2100 (Thomas et al. 2005). Concerns about the high atmospheric concentration of GHGs and the subsequent climate impacts have greatly impacted the outlook for our energy future. Three main strategies have been outlined by the US Department of Energy to limit the amount of  $CO_2$  produced (DOE & NETL, 2007).

- 1. Increase energy efficiency of transmission grids and consumer products;
- 2. Increase use of carbon-free power generation including renewable and nuclear sectors; and
- 3. Refine and implement CCS technologies for fossil fuel power generation.

Efficient CCS technologies would allow for the continued use of cheap, abundant fossil fuels for power generation in the United States and abroad for decades of reduced or negligible CO<sub>2</sub> emissions as carbon-free power generation methods are developed. Initial CCS storage assessments focused on saline aquifers and depleted oil and natural gas fields (Thomas et al. 2005). These sedimentary options allow for the storage of supercritical CO<sub>2</sub> at depths of several hundred meters or more with physical trapping mechanisms preventing the CO<sub>2</sub> from escaping. However, careful future site selection is necessary to ensure the immobilization of CO<sub>2</sub> over geologically significant time scales (Gale, 2001).

More recently, geochemical trapping has been examined as a possible method of CCS. This

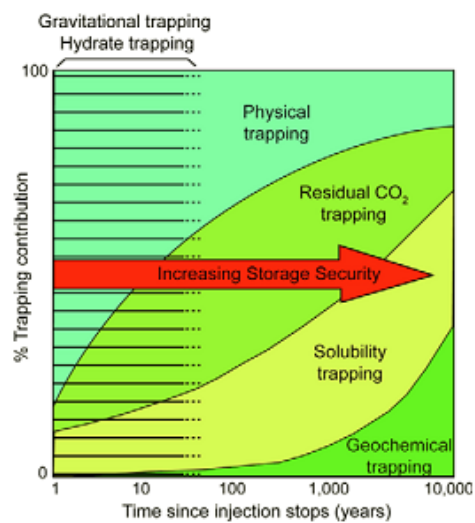


Figure 2 CO<sub>2</sub> Trapping Mechanism Stability Lin, (2007).

involves the injection of CO<sub>2</sub> into water within cavities of mafic rocks. Primary reaction products include magnesite and calcite from the release of divalent cations to the water. This method of storage offers some advantages over the sedimentary basins initially proposed. Firstly, the produced carbonates are known to be stable over geologic time scales and catastrophic release to the atmosphere is a nonissue. Secondly, this reaction is thermodynamically favorable (exothermic) and occurs spontaneously, though naturally at much slower rates as part of the global carbon cycle. Not unlike the sedimentary structures proposed for storage, mafic formations such as basalt are located worldwide both on and offshore and are currently being evaluated for injection and storage practicality (McGrail 2005).

Mineral carbonation was first proposed by Seifritz in 1990, though true development did not occur until 1995 at Los Alamos National Laboratory (Krevor, 2009). Mafic and ultramafic rocks are present in large quantities in subsurface environments worldwide. The ability of basalts and other ultramafics to sequester CO<sub>2</sub> effectively has been examined in some scientific works such as Bailly, 2004 and McGrail et al., 2006. Several laboratory studies focus on the dissolution rates of cations and the carbonate precipitation rates rather than CO<sub>2</sub> capture yield (Goldberg, 2008).

Garcia et al. (2010) performed laboratory trials with powdered olivine under a variety of grain sizes (20-200um), salinity conditions, durations (2-8 weeks), and solid/solution ratios (0-10). All trials were performed at  $150^{\circ}$  C and 150 bar. They found that up to 57% +/-2% of the initial  $CO_2$  could be captured within relatively short time frames (2-4 weeks) and that olivine and other mafic and ultramafic rocks need further examination for  $CO_2$  sequestration but show great promise. See chart in appendices for complete Garcia et al. (2010) results.

Many CO<sub>2</sub> sequestration projects are in progress worldwide. The Norwegian company Sleipner has been injecting

Project **Date Begun** Leader Location CO2 Source **Injection Site** North Sea; offshore NG Deep Saline Sleipner 1996 Statoil Norway **Processing** Formation Pan Coal Weyburn 2000 Canadian Saskatchewan, Canada Gasification FOR Depleted NG NG 2004 In Salah ΒP Algeria **Processing** Reservoir Barents Sea; offshore NG Deep Saline Snovit 2008 Statoil Norway **Processing Formation** 

CO<sub>2</sub> in the North Sea since 1996, and is currently

Table 1  $CO_2$  Programs capturing > 1 Mt  $CO_2$  annually. NG is natural gas, EOR is enhanced oil recovery.

injecting at a rate of 1 Mt per year, roughly 1/42 of their annual emissions as a nation (Johnson, 2010). In Canada, Weyburn has begun a CO<sub>2</sub> monitoring project to determine behavior and groundwater interaction. The CarbFix program in Iceland is preparing to begin storing CO<sub>2</sub> captured from a geothermal power generation plant in basalt on the island. Injection should begin during summer of 2011 (CarbFix, 2009). Enhanced oil recovery has injected CO<sub>2</sub> into oil fields to boost output, though it is generally recovered and reused and not permanently stored.

The advantage of carbonate mineralization as opposed to sedimentary sequestration is the combination of capture mechanisms that are at work simultaneously: structural trapping, hydrodynamic trapping (at depths > 700m), and mineralization (McGrail, 2006). Silicate weathering occurs naturally in both salt and fresh water systems, as bodies of water are equilibrated with atmospheric of  $CO_2$  as a system of dissolved  $CO_2$ ,  $HCO_3^-$ , and  $CO_3^{2-}$  (carbon dioxide, bicarbonate, and carbonate ion respectively). Henry's Law relates the concentration of a gas dissolved in water to the partial pressure of the gas at a given temperature. The general equation is:  $p = k_h *c$ , where p is the partial pressure of the gas, c is the concentration in water,

and k<sub>h</sub> is the Henry's law constant which depends on the gas in question and temperature of solution.

pH dictates the balance of these three components, but the acidic components weather silicate minerals and cause the release of divalent cations, which are positive atoms missing two electrons from a complete outer shell. The higher the pCO<sub>2</sub> of the system, the more CO<sub>2</sub> is dissolved and the more acidic the system (if no other pH constraints exist). For the supercritical CO<sub>2</sub> in this research, pH is on the order of 3.5, which facilitates the mobilization of metal cations, and the precipitation of carbonate thereafter (Garcia et al, 2010). The general equation is as follows:  $ASiO3 + CO_2 \rightarrow ACO_3 + SiO_2$ , where A represents a divalent cation such as magnesium, calcium, or iron.

Specific reactions are shown below, as duplicated from McGrail et al. (2010). The first reaction details the dislocation of metal cations from the basalt through reaction with hydrogen ions and water. The second reaction shows how the metal cation reacts with aqueous bicarbonate ion to form the carbonate mineral.

- 1)  $(Ca, Mg, Fe)Si_3AlO_8 + H^+ + 4H_2O \rightarrow (Ca, Mg, Fe)^{+2} + 3H_4SiO_4 + Al^{+3}$ 2)  $(Ca, Mg, Fe)^{+2} + HCO_3^- \leftrightarrow (Ca, Mg, Fe)CO_3 + H^+$

# Method of Analysis and Hypotheses

In this study, the effect of grain size on CO<sub>2</sub> sequestration rate was observed. Three different grain size ranges were studied: 425-250um, 250-180um, and <180um.

Decreasing grain size presented a larger surface area presented for reaction; this caused reaction rates of heterogeneous chemical reactions to increase. The difference in the liquid/solid interface area produced a change in the rate of precipitation with the smaller grains sequestering more CO2 in a given time span. This was due to increased dissolution because of the larger surface exposed to the solution. Each halving of



Figure 3 Sample of vesicular basalt

average grain size doubled the surface area for the same mass of sample.

	Average Grain	Surface Area per	Volume per	Mass per grain	# grains in 10	Surface area in 10
Trial	size (um)	Grain (um^2)	grain (um^3)	(arbitrary)	mass units	mass units
1	337.5	357779	20128302	20128.30	0.0004968	177.7
2	215	145192	5203567	5203.56	0.001921	279.0
3	160	80409	2144597	2144.59	0.004662	374.9

Table 2 Relationship between surface area and grain size.

The basalt sample was provided by B. Tattitch and originated in the Boring Lava field in Washington State. Literature on the Boring Lava field reveals that the mineralogy is predominantly light-gray phyric olivine basalt, with scoria, cinders, tuff, and ash all present on

the surface (USGS). As with most extrusive mafic rocks, there is a small amount of glass present in the sample. Glass dissolves and releases divalent cations more quickly in acidic aqueous solution than the other non-glassy mineral crystals such as feldspar, olivine, and pyroxene. The higher the glass content of the sample, the more CO<sub>2</sub> will be sequestered as the release of cations is the limiting step of these multipart reactions (McGrail, 2006). This basalt sample contained between 5-10% glass, and, although heterogeneous glass distribution in different grain sizes after crushing is a concern, it was out of the scope of this experiment.

The composition of the sample was determined via X-Ray Fluorescence Spectroscopy (XRF) by Dr. Stanley Mertzman at Franklin and Marshall College. This analysis was performed on a 5 gram <180um sample drawn at random from the total powdered basalt volume. The main oxides of concern to this study were those of calcium and magnesium, which form calcite and magnesite when mobilized in a CO<sub>2</sub> rich environment, respectively. The XRF revealed that these make up approximately 15.2% of the basalt sample, which is within normal ranges for basalts (McGrail, 2005). When the composition was plotted on a Total Alkali versus Silica diagram, the sample fell on the border between basalt and trachybasalt, meaning it had a higher than usual alkali content (NaO and K<sub>2</sub>O, see appendices). The total of 99.32 is not a perfect 100%, but within accepted standards. The missing 0.68 is likely due to trace elements and uncertainty in analysis.

Specimen	AF-1
SiO2	51.7
TiO2	1.19
Al2O3	17.04
Fe2O3	5.56
FeO	2.56
MnO	0.13
MgO	7.18
CaO	8.28
Na2O	3.82
K2O	1.43
P2O5	0.43
Total	99.32

Table 3 XRF sample data. All values +/- .5%.

Three hypotheses were tested to either fail under the given conditions, or be deemed consistent with the data after analysis.

- a.) H<sub>1</sub>: When ground basalt is reacted with aqueous CO<sub>2</sub> under the specified P-T conditions, stable carbonate minerals will form.
  - a.  $H_{10}$ : Carbonates will not form under the tested conditions.
- b.) H<sub>2</sub>: When different grain sizes (but identical masses) of basalt are reacted with aqueous CO<sub>2</sub>, the largest amount of carbonate will form on the sample with the smallest grains (<180um), less on the middle grain size (250-180um), and the least on the largest grain size (425-250um).
  - a.  $H_{20}$ : There will not be a significant relationship between grain size and amount of carbonate formed.
- c.) H<sub>3</sub>: The difference in the amount of carbonate formed will be smaller than the ratio of average surface areas. That is, the ratio of surface area to carbonate formed will not follow a 1:1 trend.
  - a. H<sub>3</sub><sub>o</sub>: The relationship between carbonate formed and average surface area will not follow a statistically significant trend.

The final hypothesis was added after review of the paper by Garcia et al. (2010). They found that as diameter increased (from 20-200um) and at identical test conditions, there was less carbonate formed, but it did not follow a 1:1 ratio between surface area and CO<sub>2</sub> sequestered. This study would serve to replicate these results, in addition to testing larger grain sizes and basalt in place of olivine.

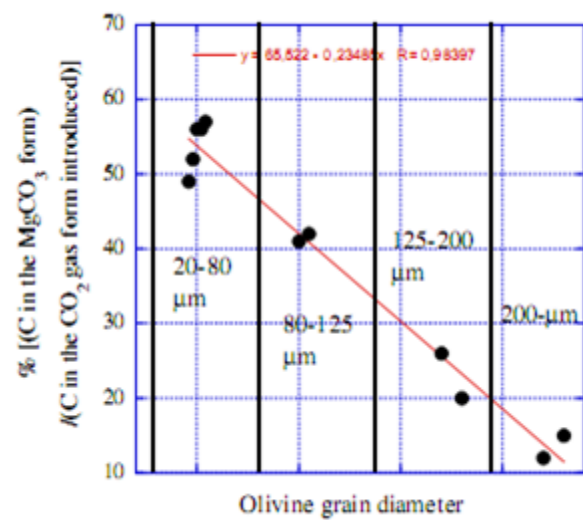


Figure 4 Percentage of CO<sub>2</sub> trapped as carbonate. From Garcia et al., 2010.

## **Experimental Design**

The basalt sample was crushed using a ceramic mortar and pestle and sieved until several grams were located between each level. Grains were sieved to the three groups mentioned earlier: 425-250um, 250-180um, and <180um. No pretreatments or washings were applied to the grains. A sample of the homogenous powder from the <180um group was used for the XRF. The materials for reaction are dry ice and distilled water of laboratory standards. The samples were reacted in stainless steel Swagelok tubing of inner diameter 0.3 cm and length of 9.678 cm, resulting in volume of 0.648 cm<sup>3</sup>. Both ends were sealed by Swagelok stainless steel pressure fittings, and the specifications for this setup are sufficient up to 260 bar (Swagelok, 2011).

Combining 0.100 gram of ground basalt, 0.100 gram of distilled water, and 0.0647g  $CO_2$  gives the appropriate internal pressure of 150 bars at an externally applied 150° C. Equal ratios of basalt and water were chosen after analysis of Garcia et al. They found that a 1:1 ratio yielded the highest carbon capture compared to both higher and lower ratios for samples of this size. The total pressure of 150 bar comprises the partial pressures of both  $CO_2$  and water. For the masses used and volume of the cylinder,  $P_{CO_2}$  is 145.3 bar and  $P_{H2O}$  is 4.7 bar. This is corrected for the initial dissolution of the gaseous  $CO_2$  and also for the volume occupied by the basalt sample. Calculation of the correct pressures and volumes involved the Law of Partial Pressures, the Antoin Equation for Vapor Pressure, and the Ideal Gas Law. Three samples of each grain size range were run at a time, for a total of nine individual trials and three 2 week periods.

As dry ice sublimes at room temperature, the powdered basalt and distilled water were first added to the Swagelok tubes, and the basalt massed, added, and quickly sealed as the final step. There is approximately a 10 second period from when the mass is recorded until the dry ice is sealed air tight inside the Swagelok vessel. Watching the mass of the dry ice change on the microbalance as it is massed gives a good idea of the rate of sublimation, and that is why the uncertainty of the dry ice mass is 0.5mg greater than the other mass uncertainties.

At the end of the two week period, the tubes were removed from the oven and allowed to cool to ambient temperature. The tubes were then opened, and the contents poured into

beakers. Distilled water was run through each tube to ensure the collection of all grains. The grains were then vacuum filtered on pre-massed filters and heated overnight at 140°C to remove any water content; sufficient for samples this minute. The dried grains and filters were then massed to determine the total mass increase from before and after reaction.

After mass difference analysis was complete, the Elemental Analyzer was used to determine the abundance of C within each sample. Each sample was run in triplets, and one sample of three trials of non-reacted powdered basalt was included, for a total of 30 samples. 8 urea standards were used for accuracy.

Setting up the Elemental Analyzer includes filling and installing combustion and reduction columns filled with specific materials for C and N analysis (O and S analyses are also performed on this machine). The combustion column contains cobaltous oxide, silica chips and silica wool, and chromium oxide. The reduction column contains the same silica chips and silica wool and copper wire. The standard used was urea as only carbon abundance is of interest to this study.

When performing runs with the Elemental Analyzer, it is important to have an appropriate amount of standards included based on the number of samples. The rough proportion is about 1 standard for every 3 samples being run, but the more standards included the higher precision the measurements will be. Also important is that the peak heights of C for the samples are similar (same order of magnitude at a minimum; ideally within 10%) to the peak heights for the standards, and that they occur at the same time. The times for the carbon peak for these samples and standards all fell within a 1 second range, averaging 234.8 seconds.

Since the carbon content is not likely to be identical between standards and samples, the masses of samples (and sometimes standards) are adjusted to keep these heights similar. The masses of basalt tested ranged from 1-8mg, while only 60ug of standard was needed. This was because the urea had between 30-60 times the carbon content of the carbonated basalt per unit mass. Masses of samples were adjusted twice based on inconclusive data until the correct peak heights were observed, and a different mass of each individual samples was used. See attached sheet in appendices for additional mass information.

# **Presentation of Data**

Group	Trial	Basalt Mass (mg) +/- 0.020	CO2 Mass (mg) +/- 0.520	H2O Volume (ml) (+/-) 0.3 uL	Filter Mass (mg) +/- 0.020	Dried Filter and Sample (mg) +/- 0.020	Mass Increase (mg) +/- 0.020	% Mass Increase
425-250um	1	101.617	66.840	0.100	457.419	563.187	4.151	4.085
425-250um	2	100.017	67.040	0.100	483.362	586.243	2.864	2.864
425-250um	3	101.064	71.060	0.100	472.487	579.034	5.483	5.425
250-180um	1	100.207	64.750	0.100	472.346	577.649	5.096	5.085
250-180um	2	100.440	68.450	0.100	481.249	588.371	6.682	6.653
250-180um	3	100.018	74.910	0.100	459.698	566.875	7.159	7.158
<180um	1	100.736	72.600	0.100	481.265	588.652	6.651	6.602
<180um	2	101.594	68.970	0.100	480.867	590.471	8.010	7.884
<180um	3	100.932	67.860	0.100	461.352	569.237	6.953	6.889

Table 4 Masses of reactants and products, and mass difference analysis.

		0/ 84===	Average	Chair	Average	A.,	Dalativa
		% Mass	Mass	Stan.	Grain Size	Average SA	Relative
Group	Trial	Increase	Increase	Dev.	(um)	(unitless)	SA
425-250um	1	4.085	4.125	1.281	337.5	177.75	1
425-250um	2	2.864			337.5	177.75	1
425-250um	3	5.425			337.5	177.75	1
250-180um	1	5.085	6.299	1.081	215	279.03	1.56
250-180um	2	6.653			215	279.03	1.56
250-180um	3	7.158			215	279.03	1.56
<180um	1	6.602	7.125	0.673	160	374.94	2.10
<180um	2	7.884			160	374.94	2.10
<180um	3	6.889			160	374.94	2.10

Table 5 Calculations and analyses of mass data

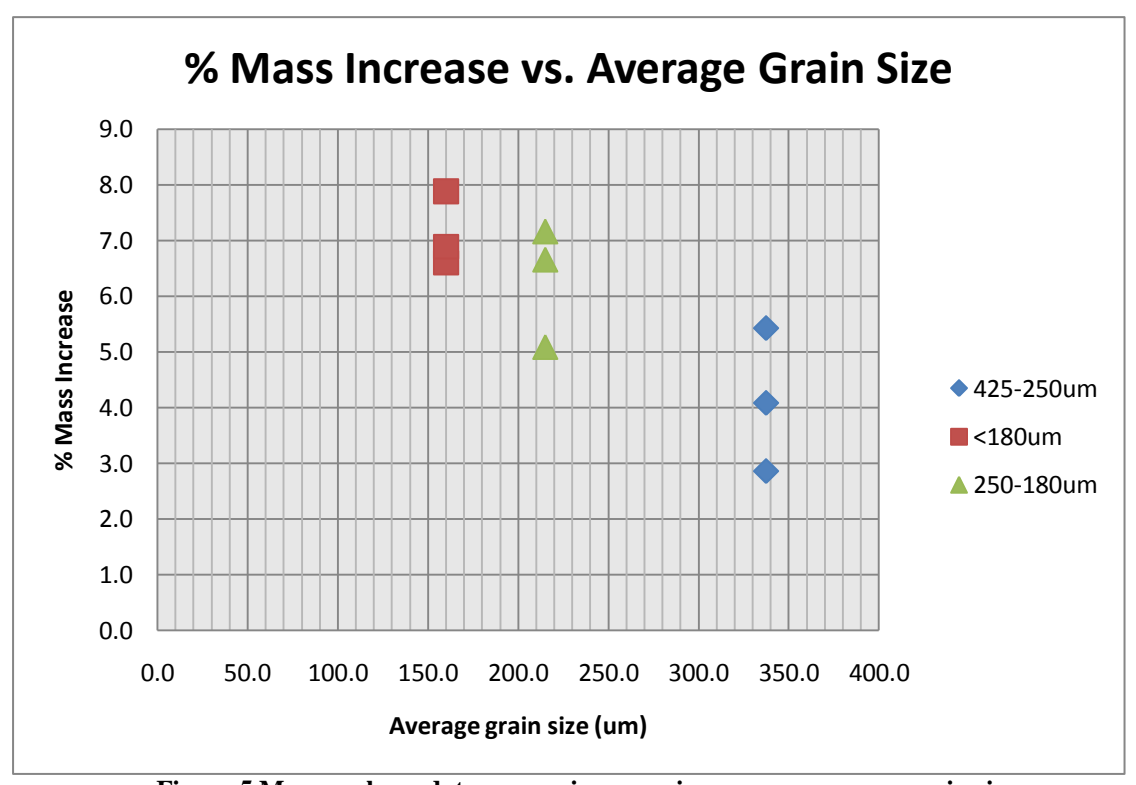


Figure 5 Mass analyses data comparing mass increase vs. average grain size. Average grain sizes calculated were 337.5um, 215um, and 160um.

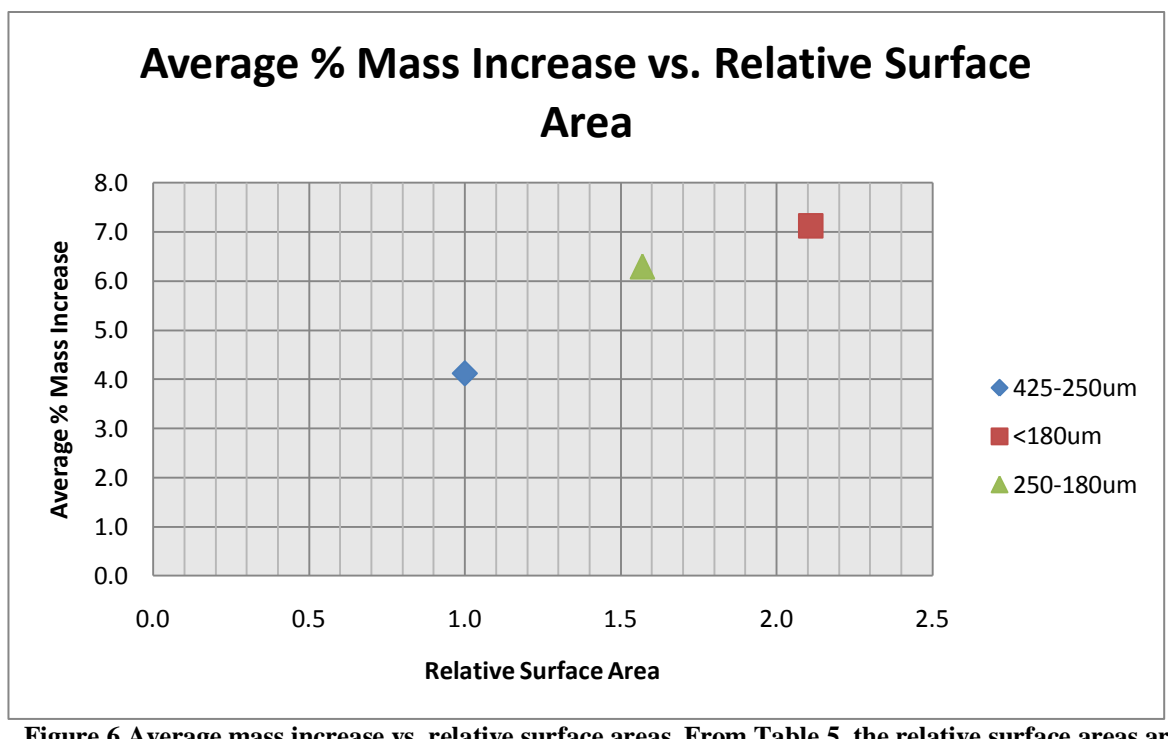


Figure 6 Average mass increase vs. relative surface areas. From Table 5, the relative surface areas are 2.11:1.57:1

									AVG C%	
									of Grain	STD DEV of
Grain size	Name	RT (Sec)	Height (nA)	Туре	Mass (mg)	Elem. Comp	AVG C%	STD DEV	size/All Stan.	Grain Size/ All Stan.
N/A	STD-2.raw	234.6	10.52	Elem	0.06	38.77	6.85	8.45	30.20	8.906
	STD-3.raw	234.5	7.90	Elem	0.07	22.85	0.05	0.43	30.20	8.900
N/A	STD-4.raw	234.1	8.72	Elem	0.07	25.88				
N/A	ACF-1a.raw	234.7	1.98	Sample	6.65	0.06				
425-250um	ACF-1b.raw	234.6	1.98	Sample	7.00	0.06	0.08	0.025	0.07	0.022
425-250um	ACF-1c.raw	234.6	3.11	Sample	6.27	0.11				
425-250um	ACF-2a.raw	235.7	2.83	Sample	7.12	0.09				
425-250um	ACF-2b.raw	234.9	1.94	Sample	6.85	0.06	0.07	0.015		
425-250um	ACF-2c.raw	234.7	2.07	Sample	7.62	0.06				
425-250um	ACF-3a.raw	234.8	1.83	Sample	7.00	0.06				
425-250um				•			0.08	0.031		
425-250um	ACF-3b.raw	234.6	3.43	Sample	6.48	0.11				
425-250um	ACF-3c.raw	235.7	2.14	Sample	7.29	0.06				
<180um	ACF-4a.raw	234.5	9.18	Sample	1.38	1.42	1.48	0.059	1.48	0.0968
<180um	ACF-4b.raw	234.5	6.63	Sample	0.97	1.46				
<180um	ACF-4c.raw	234.3	8.31	Sample	1.15	1.54				
<180um	ACF-5a.raw	234.5	6.66	Sample	0.87	1.64	1.53	0.127		
<180um	ACF-5b.raw	235.3	9.10	Sample	1.25	1.56				
<180um	ACF-5c.raw	234.6	8.41	Sample	1.29	1.39				
N/A	STD-6.raw	234.2	11.79	Elem	0.06	45.84	6.85	19.97		
N/A	STD-7.raw	235.4	7.23	Elem	0.09	17.60				
<180um	ACF-6a.raw	234.7	5.80	Sample	0.83	1.49	1.44	0.107		
<180um	ACF-6b.raw	234.6	6.13	Sample	0.99	1.32				
<180um	ACF-6c.raw	234.3	8.23	Sample	1.16	1.51				
250-180um	ACF-7a.raw	234.7	4.87	Sample	1.39	0.75	0.69	0.072	0.51	0.152
250-180um	ACF-7b.raw	235.5	4.72	Sample	1.45	0.70	0.03	0.072	0.51	0.132
250-180um	ACF-7c.raw	234.9	4.67	Sample	1.64	0.61				
	ACF-8a.raw	234.9	2.94	Sample	1.59	0.39	0.20	0.091		
250-180um 250-180um	ACF-8b.raw	234.7	2.32	Sample	1.64	0.30	0.39	0.031		
	ACF-8c.raw	235.3	3.48	Sample	1.54	0.49				
250-180um	ACF-9a.raw	235.5	4.03	Sample	1.88	0.46	0.44	0.076		
250-180um	ACF-9b.raw	234.8	4.38	Sample	1.85	0.50	0.44	0.076		
250-180um	ACF-9c.raw	234.8	2.68	Sample	1.61	0.36				
250-180um	ACF-10a.raw	234.9	1.35	Unreacted	6.21	0.05				
250-180um	ACF-10b.raw	235.9	1.41	Unreacted	7.01	0.04	0.05	0.006	0.05	0.0065
250-180um	ACF-10c.raw	235.2	1.66	Unreacted	6.36	0.06				
250-180um	STD-9.raw	234.6	10.68	Elem	0.72	31.68				
N/A	STD-10.raw	234.6	9.16	Elem	0.64	30.52	30.2	0.164		
N/A		235.1				28.43				
N/A	STD-11.raw	233.1	10.35	Elem	0.78					

**Table 6 Elemental Analyzer Results.** 

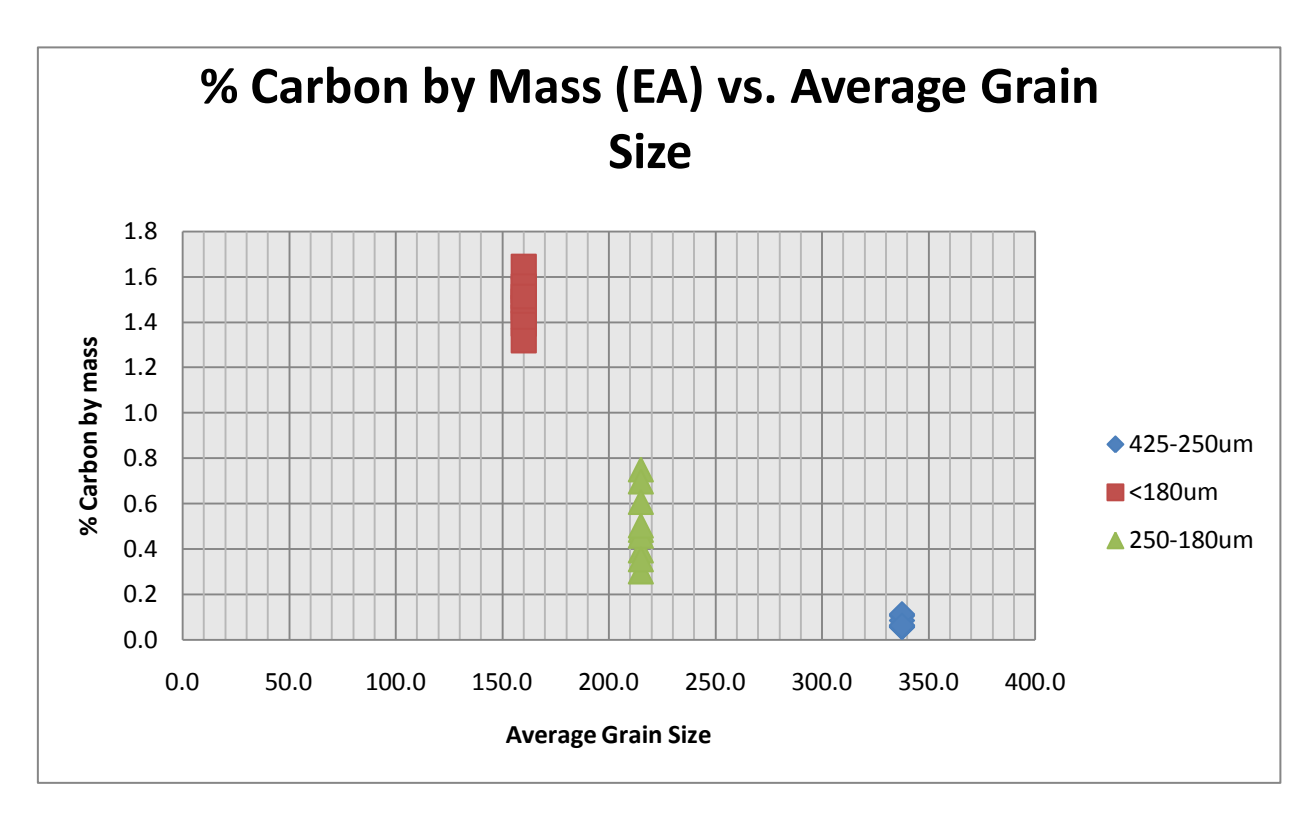


Figure 7 Average grain size vs. % carbon. Average grain sizes calculated were 337.5um, 215um, and 160um.

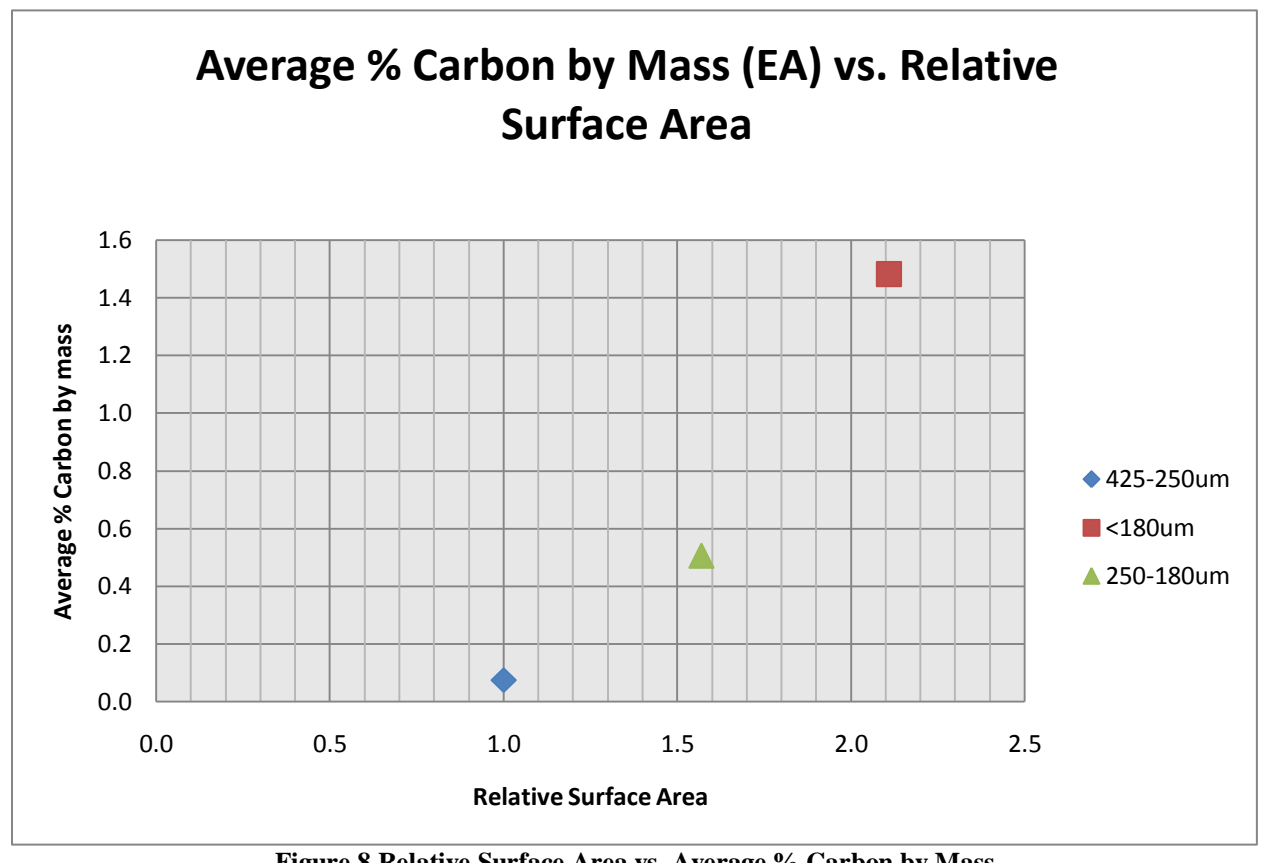


Figure 8 Relative Surface Area vs. Average % Carbon by Mass. From Table 2, the relative surface areas are 2.11:1.57:1.

#### **Discussion of Results**

At the end of the experiments, carbon was to be found in two states: unreacted gaseous CO<sub>2</sub>, and as newly formed carbonates. The gaseous CO<sub>2</sub>was not quantified in these experiments, but the yield of carbonates is. By analyzing the mass differences and Elemental analyses together, much insight can be gained into how much carbon is stored by each trial.

A direct relationship is discovered between grain size and carbon captured. Looking at the mass difference data, the largest mass increase was found in the <180um group, less on the 250-180um group, and the least on the 425-250um group. Mass increases are in the 4-7% range, which is consistent with other reactions of this duration and condition. Calculating a slope from the mass data gives m=.658, or .658 % mass increase per 1% increase in average grain size. Standard deviations range from 1.28-.673, indicating good reproducibility for these values for a sample size of only n=3. This positive correlation is reflected on figures 5 and 6, showing an increase in change in mass on the smaller average grain size and larger relative surface area.

The Elemental Analysis reveals a similar trend, but of a different magnitude. The 425-250um group again produced the lowest yield of carbon, but this time it was an order of magnitude less than the <180um group instead of approximately 58% as much. The slope for percent mass increase per percent grain size increase is m=2.16, or three times the mass analysis slope. Standard deviations for the 425-250um and <180um grain sizes are small, indication great reproducibility and very similar yields both within trials and between trials of the same grain size. The standard deviation for the 250-180um group shows less accuracy compared to the other grain sizes, but still very good for this sample size.

While the mass analyses reveal the increase in  $CO_2$ , the EA analyses reveal only the increase in carbon. Assuming all the carbon present in the samples is from newly formed carbonate, and understanding that carbon represents only 27.3% of the mass of carbonate, it is possible to extrapolate the carbonate. After calculating, the 425-250um group has an average carbonate content of .293% by mass, the 250-180um group has an average carbonate content of 1.87% by mass, and the <180um has an average carbonate content of 5.42% by mass. This is a similar trend to the respective 3.9%, 5.9%, and 6.6% respective carbonate masses of the mass analyses but smaller on all grain sizes and with a significant difference in the ratio of carbonate formed.

The cause of this discrepancy could be many reasons. One reason could be weathering of the carbonates before they were tested in the elemental analyzer. The 425-250um group was the first grain size reacted, and it remained in storage for over two months before being analyzed, as opposed to 2 weeks or less for the other two groups. The mass analyses were performed within one day of reaction for each reaction, so no storage effects would be present in those results.

Also of significant interest was the abundance of carbon revealed in the non-reacted sample. The average of .05 weight percent nearly matched the .07 weight percent of the 425-250um grain size group. This could be due to partial reaction from natural weathering processes. Rain with dissolved  $CO_2$  naturally weathers exposed and porous mafic minerals through contact. This could also be attributed to contamination, if the mortar and pestle was not perfectly clean or some other carbon source mixed with the un-reacted sample.

Both groups contain mass increases that are expected and appropriate for this type of reaction, rock, and conditions. The Garcia study saw higher yields for several reasons. The

chief reason was due to the different mineral used: pure olivine. The magnesium and iron silicate contains a much higher percentage of divalent cations ready to be released and form new minerals. Another reason is due to the way the experiment was designed. In these experiments, the pressure was internally generated and as the  $CO_2$  reacted, the pressure slowly decreased down to approximately 135 bar for the greatest sequestration yield (at  $150^{\circ}$ C, calculating using maximum  $CO_2$  sequestration analyzed). The pressure in the Garcia study was externally applied by an autoclave.

## **Analysis of Uncertainty**

<b>Uncertainties</b>	Instrument	Specification	Observed
	Sartorius C2P		(+/-) 20 ug for n=10
All masses	Microbalance	(+/-) 5 ug	
	VWR 50-200uL		(+/-) .3 uL (by mass for n=10)
H20 Volume	Micropippette Model 821	(+/-) .5 uL	(., ) (,
			Not tested
Thermometer	<b>High Range Liquid Safety</b>	(+/-) .5° C	
Oven	Checked with		148-153 C
Temperature	thermometer	N/A	
	PANalytical X'pert Pro x-	1% on major	Not tested
XRF Data	ray diffractometer	elements	
C Abundance	<b>Eurovector EA Elemental</b>	Dependent on	Not tested
Data	Analyzer	sample size	

Table 7 Uncertainty values for instruments used during trials.

The above values give the uncertainties for the instruments used during trials. However, there are also other significant uncertainties that could have had an effect on the results. Some of the ways that mass analysis could have been affected:

- Some basalt grains remain in tube or lost during vacuum filtration
- Filter was wet/dirty when initially massed
- Unequal composition of basalt
  - o Lower yield of divalent cations/more silica
  - o Higher or lower amounts of glass
- Massing/human error

Most of these uncertainties would decrease the amount of mass difference and give a lower yield than actually occurred. Extreme care and precaution was taken to prevent any loss or contamination of grains during the filtration, drying, and massing processes.

Oven temperature was controlled with a dial such as on a hot plate. Temperature was controlled by observation and adjustment with the high range liquid safety thermometer. Temperature was observed to range from 148-153° C, so including thermometer uncertainty the total range is 147.5-153.5° C for all trials.

## **Suggestions for Future Work**

As CCS and mineral carbonation sequestration are both technologies undergoing significant research, there are many questions left to answer. Laboratory work such as this is of limited use to actual injection scenarios, and is only helpful with understanding the kinetics and chemistry of reaction. To be put into application, larger scale experiments and pilot plants need to be implemented to pave the way to future full scale deployment.

The CarbFix project in Iceland should give a better look at larger scale injection sites and carbon dioxide stability. Several monitoring wells are set up around the injection area to understand the reactions occurring and the time frames (CarbFix, 2009). There are currently 31 medium scale CCS power plant projects planned for the next 5 years, with 6 pilot projects currently underway to improve the capture processes. There are also a significant amount of non-power industry CCS projects from the industrial and cement manufacturing trades.

Site	Location	Reservoir	Reservoir type	Permeability	Seal type	Start
		class				date*
Sleipner	Norway	Offshore Saline Fm.	Deep-water Sandstone	V. high	Thick shale	1996
Weyburn	Canada	Onshore EOR	Ramp carbonate	Moderate	Evaporate	2000
In Salah	Algeria	Onshore Sandstone	Fluvial/tidal sandstone	Low	Thick shale	2004
FutureGen	US	Onshore Saline Fm.	Fluvial sandstone or shelf carbonate	Moderate	Thick shales or evaporites	2012
ZeroGen	Australia	Onshore EOR/Saline	Fluvial/deltaic sandstone	Low- moderate	Shale	2011
Snohvit	Norway	Offshore Saline Fm.	Fluvial sandstone	Moderate	Shale/evap.	2008
DF1/Miller	UK	Offshore EOR	Deep-water sandstone	Moderate - high	Thick shale	2011
DF2/Carson	US	Onshore EOR	Deep-water sandstone	Moderate - high	Thick shale	2012
Latrobe Valley/ Monash	Australia	Offshore EOR/Saline	Fluvial/deltaic sandstone	High	Thin and thick shales	2011
Gorgon	Australia	Offshore Saline Fm	Deep-water sandstone	Moderate	Thick shales	2009
Hauten/ Draugen	Norway	Onshore/ Offshore Saline Fm.	Deep-water sandstone	High - V. high	Thick shales	2010
Phase III Regional Partnerships	US	Varying, but mostly Saline Fm.	Varying	Varying	Varying	2010

\* = date of first injection or planned first injection of CO2

Table 8 Locations of future and current large scale CO<sub>2</sub> injection site from Friedmann (2007).

#### **Conclusions**

- a.) H<sub>1</sub>: When ground basalt is reacted with aqueous CO<sub>2</sub> under the specified P-T conditions, stable carbonate minerals will form.
  - a. H<sub>10</sub>: Carbonates will not form under the tested conditions.

Both the elemental and mass analyses revealed significant increases in the mass and carbon content of the basalt samples.  $H_{1o}$  is proven incorrect, and  $H_{1}$  is tentatively deemed to be consistent with the results of these experiments.

- b.) H<sub>2</sub>: When different grain sizes (but identical masses) of basalt are reacted with aqueous CO<sub>2</sub>, the largest amount of carbonate will form on the sample with the smallest grains (<180um), less on the middle grain size (250-180um), and the least on the largest grain size (425-250um).
  - a. H<sub>20</sub>: There will not be a significant relationship between grain size and amount of carbonate formed.

Though differing by an order of magnitude, both the elemental and mass analyses revealed the largest mass increase and carbon abundance on the <180um grain size group, less on the 250-180um grain size group, and the least on the 425-250um group. As these differences show reproducibility and significant standard deviations,  $H_{20}$  is proven incorrect, and  $H_{2}$  is tentatively deemed to be consistent with the results of these experiments.

- c.) H<sub>3</sub>: The difference in the amount of carbonate formed will be smaller than the ratio of average surface areas. That is, the ratio of surface area to carbonate formed will not follow a 1:1 trend.
  - a. H<sub>30</sub>: The relationship between carbonate formed and average surface area will not follow a statistically significant trend.

As the elemental and mass analyses data show similar trends but strongly different slopes, including one slope above 1:1 and one below 1:1, there is not enough data to refute  $H3_0$  and  $H_3$  is deemed to be inconsistent with the data recorded.

## **Discussion**

Validation and reproducibility are important concepts in the scientific community. To perform similar experiments as the Garcia et al. paper, with a different rock type, is an interesting and valuable corollary to the growing library of CCS related geological knowledge. This study aids in the understanding of dissolution and precipitation rates for basalts in CO<sub>2</sub> rich conditions. With a better understanding in this area, quantitative storage and cost estimates can be refined and, eventually, large mW scale trials will be underway.

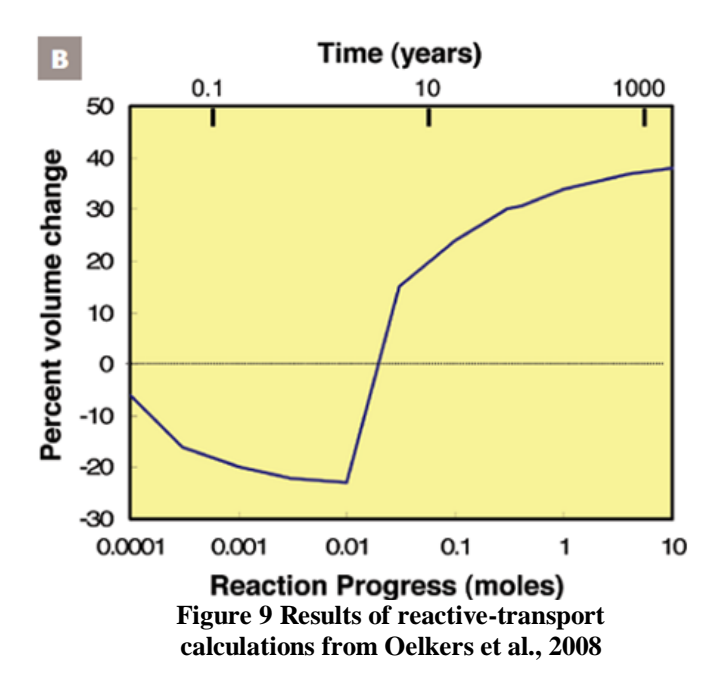
Foundational research for any new technology requires significant time and expense commitments. CCS is an immature technology, and the mineral trapping techniques have only recently begin to receive the attention and funding deserved.

A reduction in the CO<sub>2</sub> released from major point sources in the USA will allow for continued use of cheap, abundant, reliable fossil fuels. As the energy industry is making slow strides toward carbon free power generation, the CCS technologies such as geochemical trapping and other geologic storage options could extend the operational lifetime of our fossil fuel power plants. Although new fossil fuel plants may not be built to support future demand increases, the ability to be retrofitted to existing fossil fuel generation plants offers flexibility as alternate energy methods are developed and added to the current grid.

These amounts of mass increases are enough that useful judgments can be made, but not enough to store significant amounts of carbon dioxide. The reactions at injections sites will be

at lower pressures and temperatures (on the order of  $70^{\circ}$ C and 70 bar), and the reactions will take orders of magnitude more time. The carbon dioxide will be permeating the rock for thousands of years due to physical trapping, leavings plenty of time for the reaction to occur (McGrail et al, 2005).

When injecting carbon dioxide into a basaltic aquifer at 60°C and 100 bars, the volumetric changes that occur are perhaps unexpected. There is a net volume loss over the first 7 years that maximizes at 20% due to dissolution reactions. After this point the precipitation becomes dominant reaction and begins filling pore spaces, reaching 40% filled by 1000 years after injection. Concerns over clogging the porous and permeable basalt flow tops are therefore unfounded, as it takes >5 years for precipitation to overtake dissolution and provides a significant window for injection (Oelkers et al, 2008).



# Acknowledgements

It is a pleasure to participate in research in such a young field and keep up with advancements as they occur. My work would not have been possible without the work of those before me, on whose shoulders I stand. Most helpful was the work of Garcia et al., David S. Goldberg, and McGrail et al., leading authorities in the basalt sequestration area.

Those who have been great help personally include:

- MN Evans UMD
- Yongbo Peng UMD
- Jay Kaufman UMD
- Brian Tattitch UMD
- Nick Gava UMD
- Sarah Peek UMD
- Grant Jiang UMD
- Philip Candela UMD
- Natalie Sievers UMD
- Karen Obenshain EEI
- Madalyn Blondes USGS
- Nick Woodward DOE

## **Bibliography**

- Beecy D. Status of U.S. geologic carbon sequestration research and technology. Environmental Geosciences. September 1, 2001;8(3):152-159. Available from: GeoRef, Ipswich, MA. Accessed September 30, 2010.
- Bradshaw J. Environmental Geosciences CO<sub>2</sub> sequestration. Environmental Geosciences. September 1, 2001;8(3):149-224. Available from: GeoRef, Ipswich, MA. Accessed September 30, 2010.
- CarbFix CO2 Fixation into Basalts. "Annual Status Report 2009." Hólmfríður Sigurðardóttir.
- Chiaramonte L. Seal integrity and feasibility of CO<sub>2</sub> sequestration in the Teapot Dome EOR pilot; geomechanical site characterization. Environmental Geology [Berlin]. June 1, 2008;54(8):1667-1675. Available from: GeoRef, Ipswich, MA. Accessed September 30, 2010.
- Department of Energy Office of Fossil Energy. National Energy Technology Laboratory. "Carbon Sequestration Technology Roadmap and Program Plan." 2007. <a href="http://www.netl.ndoe.gov/technologies/carbon\_seq/refshelf/project%20portfolio/2007/2007roadmap.pdf">http://www.netl.ndoe.gov/technologies/carbon\_seq/refshelf/project%20portfolio/2007/2007roadmap.pdf</a>.
- Duan, Zhenhao. "An improved model calculating CO<sub>2</sub> solubility in pure water and aqueous NaCl solutions from 273 to 533 K and from 0 to 2000 bar." Chemical Geology 193.3-4 (2003): 257-271. GeoRef. EBSCO. Web. 12 Nov. 2010.
- Friedmann, S.J. "Carbon Capture and Storage." Oxford Companion to Global Change. Lawrence Livermore National Laboratory. October 4, 2007. UCRL 235276.
- Gale, J. "Demonstrating the potential for geological storage of CO<sub>2</sub>; the Sleipner and GESTCO projects." Environmental Geosciences. September 1, 2001;8(3):160-165. Available from: GeoRef, Ipswich, MA. Accessed September 30, 2010.
- Galle, O. Karmie. "Determination of CO<sub>2</sub> in carbonate rocks by controlled loss on ignition." Journal of Sedimentary Petrology 30.4 (1960): 613-618. GeoRef. EBSCO. Web. 23 Nov. 2010.
- Garcia, B. "Experiments and geochemical modelling of CO<sub>2</sub> sequestration by olivine; potential, quantification." Applied Geochemistry 25.9 (2010): 1383-1396. GeoRef. EBSCO. Web. 11 Nov. 2010.
- Goldberg, D. Carbon dioxide sequestration in deep-sea basalt. Proceedings of the National Academy of Sciences. July 22, 2008; 105(29):9920-9925. Available from: GeoRef, Ipswich, MA. Accessed September 30, 2010.
- Haywood H. Carbon dioxide sequestration as stable carbonate minerals; environmental barriers. Environmental Geology [Berlin]. November 1, 2001;41(1-2):11-16. Available from: GeoRef, Ipswich, MA. Accessed September 30, 2010.

- Heiri, Oliver. "Loss on ignition as a method for estimating organic and carbonate content in sediments; reproducibility and comparability of results." Journal of Paleolimnology 25.1 (2001): 101-110. GeoRef. EBSCO. Web. 23 Nov. 2010.
- Johnson, James. A Solution for Carbon Dioxide Overload. www.llnl.gov/str//Johnson.html.
- Lewis C. Global warming; an oil and gas company perspective; prospects for geologic sequestration?. Environmental Geosciences. September 1, 2001;8(3):177-186. Available from: GeoRef, Ipswich, MA. Accessed September 30, 2010.
- Lin H. Investigation of interactions in a simulated geologic CO<sub>2</sub>/rock minerals system for CO (sub 2) underground sequestration. AIP Conference Proceedings . January 1, 2007;898:17-21. Available from: GeoRef, Ipswich, MA. Accessed September 30, 2010.
- McGrail, B. Peter. "Potential for carbon dioxide sequestration in flood basalts." Journal of Geophysical Research 111.B12 (2006): @B12201. GeoRef. EBSCO. Web. 28 Apr. 2011.
- McGrail, B. Peter. "Carbon sequestration in flood basalts; an overlooked sequestration option." Abstracts: Annual Meeting American Association of Petroleum Geologists 14.(2005): A90. GeoRef. EBSCO. Web. 28 Apr. 2011.
- McGrail, B. Peter. "Use of forced mineral trapping for sequestration of CO<sub>2</sub>. " (2001): GeoRef. EBSCO. Web. 28 Apr. 2011.
- Meehl, G.A., et al. 2007: Global Climate Projections. "Climate Change 2007: The Physical Science Basis." Contribution of Working Group I to the Fourth Assessment Report of the Intergovernmental Panel on Climate Change. Cambridge University Press, Cambridge, United Kingdom and New York, NY, USA. Accessed 4/20/11.
- Oelkers E. Carbon dioxide sequestration; a solution to a global problem. Elements. October 1, 2008;4(5):305-310. Available from: GeoRef, Ipswich, MA. Accessed September 30, 2010.
- Oelkers, E. Mineral Carbonation of CO<sub>2</sub>. Elements, October 1, 2008;4(5):333-337. Available from: GeoRef, Ipswich, MA. Accessed September 30, 2010.
- Saripalli, K. Prasad. "Modeling the sequestration of CO <sub>2</sub> in deep geological formations." (2001): GeoRef. EBSCO. Web. 28 Apr. 2011.
- Sasaki K. Numerical simulation of injection for CO<sub>2</sub> geological sequestration with a treatment of CO (sub 2) dissolution into water. AIP Conference Proceedings. January 1, 2007;898:45-52. Available from: GeoRef, Ipswich, MA. Accessed September 30, 2010.

- Shaffer, G. Long-term effectiveness and consequences of carbon dioxide sequestration. Nature Geoscience. July, 2010;3:464-467. Available from: GeoRef, Ipswich, MA. Accessed September 30, 2010.
- Swagelok. "Stainless Steel Tubing and Accessories Catalog." www.swagelok.com. 4/27/11.
- Thomas, D. "Carbon Dioxide Capture for Storage in Deep Geologic Formations." 1st ed. Vol. 1. Elsevier, 2005. 6 July 2006. Web. 28 Apr. 2011. <a href="http://books.google.com/books?id=9GjBxoOqqFAC&>">http://books.google.com
- USGS. "Description: The Boring Lava Field." Updated 05/01/07. Accessed 04/22/11. http://vulcan.wr.usgs.gov/Volcanoes/Oregon/BoringLavaField/description\_boring\_lava.html.

# **Appendices**

Garcia et al. (2010) data from powdered olivine reactions.

Table 1

Initial conditions and results of the experiments conducted with olivine powders at 150 °C and 150 bar, for different grain diameters and different time reaction. Carbon dioxide in the gas form (1) (GC-analyses) and trapped in carbonate phase (2) (Rock-Eval 6 analyses). Ratios of C in the carbonate phase over C in the CO<sub>2</sub> gas form initially introduced are expressed in an our correspond to "carbonation yields". Carbon mass balances are expressed in percentage.

Initial condit	Experiment Time Grain Mass Solution Mass of CO <sub>2</sub>					CO:	CO <sub>2</sub> (retrieved as gas after	Quantity of CO <sub>2</sub> trapped as	MagC ratio: [(C in the XCO <sub>3</sub>	C-mass balance
Experiment	(weeks)	diameter (µm)	of olivine (mg)	Solution	solution (mg)	(introduced as gas) (mg eqC)**	reaction) mg eqC <sup>a</sup>	carbonate (mg eqC) <sup>b</sup> in the XCO <sub>3</sub> form	form)/(C in the CO <sub>2</sub> gas form introduced)] (%)	(%)
E-01	2	20 < d < 80	102.7 ± 0.1	1	0	30.5 ± 0.8	28.7 ± 0.4	$0.0 \pm 0.1$	$0.0 \pm 0.1$	94 ±
E-02	2	20 < d < 80	$98.5 \pm 0.1$	1	0	27.6 ± 0.7	25.2 ± 0.3	$0.0 \pm 0.1$	$0.0 \pm 0.1$	91 ±
E-03	4	20 < d < 80	$98.0 \pm 0.1$	1	0	27.1 ± 0.5	26.2 ± 0.3	$0.0 \pm 0.1$	$0.0 \pm 0.1$	97 ±
E-04	4	20 < d < 80	99.2 ± 0.1	1	0	26.4 ± 0.3	25.1 ± 0.4	$0.0 \pm 0.1$	$0.0 \pm 0.1$	95 ±
E-05	2	20 < d < 80	$102.9 \pm 0.1$	Ultra-pure water	$100 \pm 0.2$	14.5 ± 0.2	$7.1 \pm 0.2$	$7.2 \pm 0.2$	49 ± 3	98 ±
E-06	2	20 < d < 80	102.7 ± 0.1	Ultra-pure water	$100 \pm 0.2$	16.4 ± 0.2	$7.6 \pm 0.2$	$7.4 \pm 0.2$	45 ± 3	91 ±
E-07	2	20 < d < 80	101,8 ± 0,1	Ultra-pure water	$100 \pm 0.2$	15.5 ± 0.2	$7.3 \pm 0.2$	$7.2 \pm 0.2$	46 ± 2	94 ±
E-08	4	20 < d < 80	100,4 ± 0,1	Ultra-pure water	$10 \pm 0.1$	$21.4 \pm 0.4$	10.7 ± 0.4	$9.2 \pm 0.2$	43 ± 2	93 ±
E-09	4	20 < d < 80	100.8 ± 0.1	Ultra-pure water	$10 \pm 0.1$	23.1 ± 0.5	11.1 ± 0.5	$9.4 \pm 0.2$	41 ± 2	89 ±
E-10	4	20 < d < 80	99.6 ± 0.1	Ultra-pure water	100 ± 0.2	22.2 ± 0.5	11.5 ± 0.5	11.0 ± 0.2	49 ± 3	101 ±
E-11	4	20 < d < 80	99.6 ± 0.1	Ultra-pure water	$100 \pm 0.2$	18.2 ± 0.3	n.m.	9.5 ± 0.2	52 ± 2	n.d.
E-12	4	20 < d < 80	102.6 ± 0.1	Ultra-pure water	$100 \pm 0.2$	19.3 ± 0.4	8.1 ± 0.2	10.8 ± 0.3	56 ± 3	98 ±
E-13	4	20 < d < 80	100.9 ± 0.1	Ultra-pure water	100 ± 0.2	24.0 ± 0.7	10.3 ± 0.5	13.5 ± 0.3	56 ± 3	99 ±
E-14	4	20 < d < 80	$98.9 \pm 0.1$	Ultra-pure water	$100 \pm 0.2$	19.4 ± 0.5	$7.9 \pm 0.2$	11.1 ± 0.2	57 ± 2	98 ±
E-15	4	20 < d < 80	100,2 ± 0,1	Ultra-pure water	1000 ± 2	21.2 ± 0.4	13.2 ± 0.5	$7.6 \pm 0.2$	36 ± 2	98 ±
E-16	4	20 < d < 80	100.7 ± 0.1	Ultra-pure water	1000 ± 2	19.8 ± 0.3	12.8 ± 0.5	6.7 ± 0.2	34 ± 2	98 ±
E-17	8	20 < d < 80	99.4 ± 0.1	Ultra-pure water	$100 \pm 0.2$	19.3 ± 0.2	8.2 ± 0.3	10.4 ± 0.2	54 ± 2	96 ±
E-18	8	20 < d < 80	98.6 ± 0.1	Ultra-pure water	$100 \pm 0.2$	19.7 ± 0.2	$8.3 \pm 0.3$	10.9 ± 0.2	55 ± 3	97 ±
E-19	8	20 < d < 80	99.1 ± 0.1	Ultra-pure water	$100 \pm 0.2$	19.9 ± 0.3	$8.9 \pm 0.3$	10.6 ± 0.2	53 ± 3	98 ±
E-20	4	80 < d < 125	100.3 ± 0.1	Ultra-pure water	100 ± 0.2	21.2 ± 0.3	11.2 ± 0.2	8.7 ± 0.3	41 ± 2	94 ±
E-21	4	80 < d < 125	101.4 ± 0.1	Ultra-pure water	$100 \pm 0.2$	24.5 ± 0.3	n.m.	10.3 ± 0.3	42 ± 2	n.d.
E-22	4	125 < d < 200	97.7 ± 0.1	Ultra-pure water	100 ± 0.2	26.0 ± 0.3	19.7 ± 0.3	6.8 ± 0.1	26 ± 2	102 ±
E-23	4	125 < d < 200	99.2 ± 0.1	Ultra-pure water	100 ± 0,2	22.4 ± 0.3	16.8 ± 0.3	4.5 ± 0.1	20 ± 2	95 ±
E-24	4	d > 200	91.2 ± 0.1	Ultra-pure water	100 ± 0.2	21.1 ± 0.3	n.m.	2.5 ± 0.1	12 ± 1	n.d.
E-25	4	d > 200	94.0 ± 0.1	Ultra-pure water	100 ± 0.2	28.9 ± 0.3	23.4 ± 0.4	4.4 ± 0.1	15 ± 1	96 ±
E-26	4	20 < d < 80	101,0 ± 0,1	NaCl (I = 1.7 mM)		22.5 ± 0.5	16.3 ± 0.5	9.3 ± 0.2	41 ± 2	113 ±
E-27	4	20 < d < 80	100.4 ± 0.1	NaCl (I = 1.7 mM)		22.1 ± 0.5	14.0 ± 0.4	8.6 ± 0.2	39 ± 2	102 ±
E-28	4	20 < d < 80	99.9 ± 0.1	NaCl (I = 1.7 mM)		22.7 ± 0.8	12.7 ± 0.5	11.8 ± 0.3	52 ± 3	108 ±
E-29	4	20 < d < 80	99.6 ± 0.1	NaCl (I = 1.7 mM)		22.3 ± 0.6	11.3 ± 0.4	11.1 ± 0.3	50 ± 3	100 ±
E-30	4	20 < d < 80	100.3 ± 0.1	NaCl (I = 1.7 mM)	1000 ± 2	21.8 ± 0.5	n.m.	8.7 ± 0.2	40 ± 2	n.d.
E-31	4	20 < d < 80	100.1 ± 0.1	NaCl (I = 1.7 mM)	1000 ± 2	23.4 ± 0.7	14.6 ± 0.5	9.1 ± 0.3	39 ± 2	101 ±
E-32	4	20 < d < 80	99.7 ± 0.1	NaCl (I = 17 mM)	10 ± 0.1	21.9 ± 0.5	n.m.	7.2 ± 0.2	33 ± 2	n.d.
E-33	4	20 < d < 80	100.7 ± 0.1	NaCl (I = 17 mM)	10 ± 0.1	22.4 ± 0.5	n.m.	7.0 ± 0.2	31 ± 2	n.d.
E-34	4	20 < d < 80	99.5 ± 0.1	NaCl (I = 17 mM)	100 ± 0.2	21.7 ± 0.3	9.9 ± 0.4	12.2 ± 0.1	56 ± 1	102 ±
E-35	4	20 < d < 80	99.3 ± 0.1	NaCl (I = 17 mM)	100 ± 0.2	22.3 ± 0.3	10.8 ± 0.5	11.6 ± 0.2	52 ± 2	100 ±
E-36	4	20 < d < 80	99.8 ± 0.1	NaCl (I = 17 mM)	1000 ± 0.2	21.1 ± 0.3	14.3 ± 0.5	6.1 ± 0.1	29 ± 1	97 ±
E-37	4	20 < d < 80	100.6 ± 0.1	NaCl (I = 17 mM)	1000 ± 2	19.8 ± 0.3	15.2 ± 0.5	5.1 ± 0.1	26 ± 1	102 ±
E-38	4	20 < d < 80	99.4 ± 0.1	Saline solution	10 ± 0.1	23.7 ± 0.8	n.m.	1.2 ± 0.1	5.1 ± 0.2	n.d.
E-39	4	20 < d < 80	100.2 ± 0.1	Saline solution	10 ± 0.1	22.4 ± 0.3	19.2 ± 0.7	1.1 ± 0.1	4.8 ± 0.2	91 ±
E-40	4	20 < d < 80	99.3 ± 0.1	Saline solution	10 ± 0.1	21.9 ± 0.3	10.8 ± 0.4	12.2 ± 0.1	56 ± 1	105 ±
E-41	4	20 < d < 80	99.8 ± 0.1	Saline solution*	100 ± 0.2	21.5 ± 0.3	n.m.	11.4 ± 0.1	53 ± 1	n.d.
E-42	4	20 < d < 80	100.0 ± 0.1	Saline solution	100 ± 0.2	11.1 ± 0.3	n.m.	2.0 ± 0.1	18.0 ± 0.6	n.d.
E-42 E-43	4	20 < d < 80	99.7 ± 0.1	Saline solution	1000 ± 2	18.9 ± 0.3	n.m.	2.8 ± 0.2	15 ± 1	n.d.

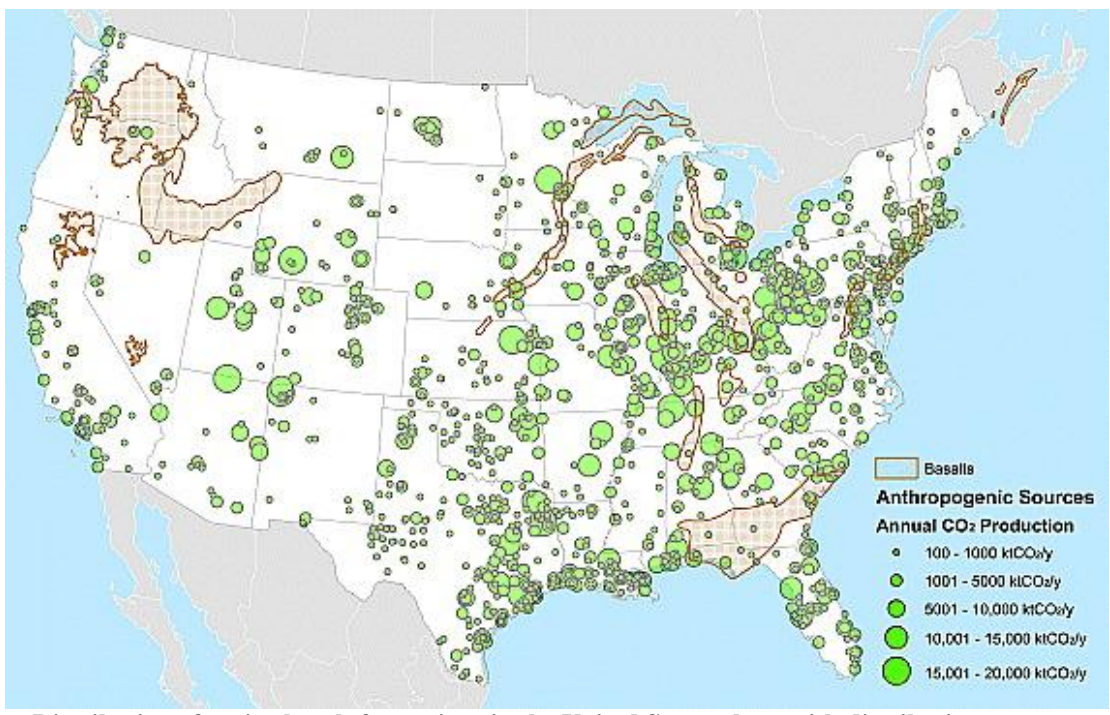
n.m.: not measured.

<sup>.</sup>d.: not detectable \* Cas analyses.

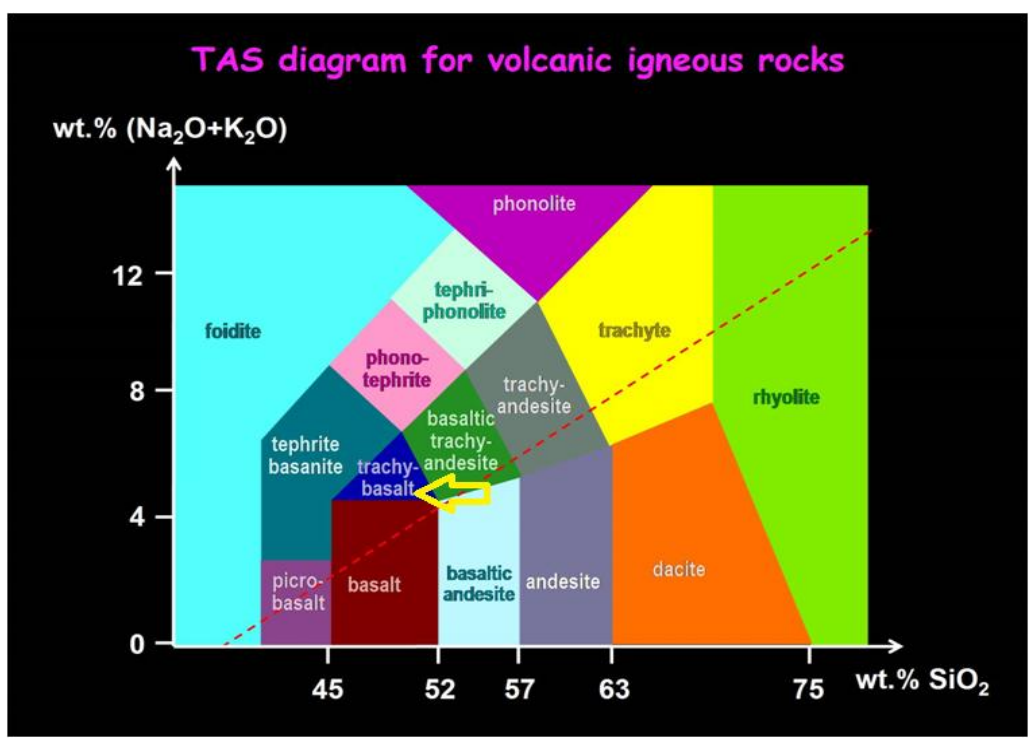
b Rock-Eval 6 analyses.

solution saline = [NaH<sub>2</sub>PO<sub>4</sub>, 2H<sub>2</sub>O (1000 mg L<sup>-1</sup>) + NH<sub>4</sub>Ol (1000 mg L<sup>-1</sup>) + NH<sub>4</sub>NO<sub>2</sub> (1000 mg L<sup>-1</sup>) + NaCl (1000 mg L<sup>-1</sup> under stoichiometric quantities).

<sup>\*\*</sup> CO2 introduced as gas (mg eqC): Dry ice CO2 was introduced in a glove box under a N2 atmosphere and then the tubes were sealed with an ultrasonic device. Masses of each tube were measured prior to and after CO2 introduction, which allowed measuring the real and precise quantity of CO2 introduced for each experiment.



Distribution of major basalt formations in the United States along with distribution of  ${\rm CO_2}$  sources. McGrail et al., 2006.



TAS Diagram showing where Boring Vesicular Basalt sample plots (point of yellow arrow)



Swagelok Stainless Steel reaction vessels, pen for scale.



**EuroVector Elemental Analyser** 





**Vacuum Filtration Apparatus** 

Basalt grain showing calcite growth after reaction with  $CO_2$  at 10.3 MPA and 90 C for 8 weeks (McGrail, 2006)

I pledge on my honor that I have not given or received any unauthorized assistance or plagiarized on this assignment.

Signed	Date